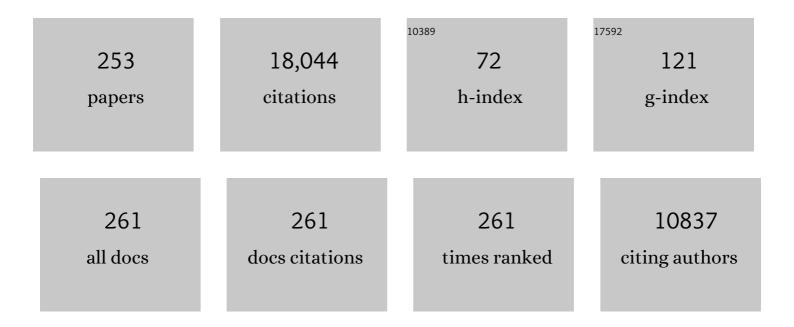
List of Publications by Year in descending order

Source: https://exaly.com/author-pdf/3879955/publications.pdf Version: 2024-02-01



#	Article	IF	CITATIONS
1	Mechanism of Nitrogen Fixation by Nitrogenase: The Next Stage. Chemical Reviews, 2014, 114, 4041-4062.	47.7	1,379
2	Beyond fossil fuelâ $\in$ "driven nitrogen transformations. Science, 2018, 360, .	12.6	1,379
3	Mechanism of Mo-Dependent Nitrogenase. Annual Review of Biochemistry, 2009, 78, 701-722.	11.1	561
4	Hydroxylation of Camphor by Reduced Oxy-Cytochrome P450cam:Â Mechanistic Implications of EPR and ENDOR Studies of Catalytic Intermediates in Native and Mutant Enzymes. Journal of the American Chemical Society, 2001, 123, 1403-1415.	13.7	442
5	Climbing Nitrogenase: Toward a Mechanism of Enzymatic Nitrogen Fixation. Accounts of Chemical Research, 2009, 42, 609-619.	15.6	336
6	Nitrogenase: A Draft Mechanism. Accounts of Chemical Research, 2013, 46, 587-595.	15.6	328
7	Reconsideration of X, the Diiron Intermediate Formed during Cofactor Assembly inE. coliRibonucleotide Reductase. Journal of the American Chemical Society, 1996, 118, 7551-7557.	13.7	253
8	Reduction of Substrates by Nitrogenases. Chemical Reviews, 2020, 120, 5082-5106.	47.7	234
9	Particulate methane monooxygenase contains only mononuclear copper centers. Science, 2019, 364, 566-570.	12.6	217
10	Ligand spin densities in blue copper proteins by q-band proton and nitrogen-14 ENDOR spectroscopy. Journal of the American Chemical Society, 1991, 113, 1533-1538.	13.7	201
11	Substrate Interactions with the Nitrogenase Active Site. Accounts of Chemical Research, 2005, 38, 208-214.	15.6	199
12	Trapping H-Bound to the Nitrogenase FeMo-Cofactor Active Site during H2Evolution:Â Characterization by ENDOR Spectroscopy. Journal of the American Chemical Society, 2005, 127, 6231-6241.	13.7	196
13	Electron-Nuclear Double Resonance Spectroscopic Evidence ThatS-Adenosylmethionine Binds in Contact with the Catalytically Active [4Feâ^'4S]+Cluster of Pyruvate Formate-Lyase Activating Enzyme. Journal of the American Chemical Society, 2002, 124, 3143-3151.	13.7	186
14	An Anchoring Role for FeS Clusters:  Chelation of the Amino Acid Moiety of S-Adenosylmethionine to the Unique Iron Site of the [4Feâ^4S] Cluster of Pyruvate Formate-Lyase Activating Enzyme. Journal of the American Chemical Society, 2002, 124, 11270-11271.	13.7	185
15	Compound ES of Cytochrome c Peroxidase Contains a Trp .piCation Radical: Characterization by Continuous Wave and Pulsed Q-Band External Nuclear Double Resonance Spectroscopy. Journal of the American Chemical Society, 1995, 117, 9033-9041.	13.7	180
16	Catalytic Mechanism of Heme Oxygenase through EPR and ENDOR of Cryoreduced Oxy-Heme Oxygenase and Its Asp 140 Mutants. Journal of the American Chemical Society, 2002, 124, 1798-1808.	13.7	159
17	Characterization of an Fe≡N–NH <sub>2</sub> Intermediate Relevant to Catalytic N <sub>2</sub> Reduction to NH <sub>3</sub> . Journal of the American Chemical Society, 2015, 137, 7803-7809.	13.7	155
18	Internal dynamics of a supramolecular nanofibre. Nature Materials, 2014, 13, 812-816.	27.5	154

#	Article	IF	CITATIONS
19	Purified particulate methane monooxygenase from Methylococcus capsulatus (Bath) is a dimer with both mononuclear copper and a copper-containing cluster. Proceedings of the National Academy of Sciences of the United States of America, 2003, 100, 3820-3825.	7.1	145
20	Hydroperoxy-Heme Oxygenase Generated by Cryoreduction Catalyzes the Formation of α-meso-Hydroxyheme as Detected by EPR and ENDOR. Journal of the American Chemical Society, 1999, 121, 10656-10657.	13.7	143
21	EPR and ENDOR of Catalytic Intermediates in Cryoreduced Native and Mutant Oxy-Cytochromes P450cam:Â Mutation-Induced Changes in the Proton Delivery System. Journal of the American Chemical Society, 1999, 121, 10654-10655.	13.7	139
22	Q-Band Pulsed Electron Spin-Echo Spectrometer and Its Application to ENDOR and ESEEM. Journal of Magnetic Resonance Series A, 1996, 119, 38-44.	1.6	138
23	Reductive Elimination of H <sub>2</sub> Activates Nitrogenase to Reduce the Nâ‰;N Triple Bond: Characterization of the E <sub>4</sub> (4H) Janus Intermediate in Wild-Type Enzyme. Journal of the American Chemical Society, 2016, 138, 10674-10683.	13.7	131
24	Metal-Ion Valencies of the FeMo Cofactor in CO-Inhibited and Resting State Nitrogenase by57Fe Q-Band ENDOR. Journal of the American Chemical Society, 1997, 119, 11395-11400.	13.7	130
25	The Metal Centers of Particulate Methane Monooxygenase from <i>Methylosinus trichosporium</i> OB3b. Biochemistry, 2008, 47, 6793-6801.	2.5	130
26	Crystal Structure and Characterization of Particulate Methane Monooxygenase from <i>Methylocystis</i> species Strain M. Biochemistry, 2011, 50, 10231-10240.	2.5	130
27	CO Binding to the FeMo Cofactor of CO-Inhibited Nitrogenase:Â13CO and1H Q-Band ENDOR Investigation. Journal of the American Chemical Society, 1997, 119, 10121-10126.	13.7	129
28	14N,1H, and metal ENDOR of single crystal Ag(II)(TPP) and Cu(II)(TPP). Molecular Physics, 1980, 39, 1073-1109.	1.7	128
29	Electron nuclear double resonance (ENDOR) of metalloenzymes. Accounts of Chemical Research, 1991, 24, 164-170.	15.6	124
30	The dioxygen adduct of meso-tetraphenylporphyrinmanganese(II), a synthetic oxygen carrier. Journal of the American Chemical Society, 1976, 98, 5473-5482.	13.7	123
31	Intermediates Trapped during Nitrogenase Reduction of Nâ‹®N, CH3â^'NNH, and H2Nâ^'NH2. Journal of the American Chemical Society, 2005, 127, 14960-14961.	13.7	122
32	The Core Structure of X Generated in the Assembly of the Diiron Cluster of Ribonucleotide Reductase:Â17O2and H217O ENDOR. Journal of the American Chemical Society, 1998, 120, 12910-12919.	13.7	119
33	Electron Transfer within Nitrogenase: Evidence for a Deficit-Spending Mechanism. Biochemistry, 2011, 50, 9255-9263.	2.5	117
34	An Organometallic Intermediate during Alkyne Reduction by Nitrogenase. Journal of the American Chemical Society, 2004, 126, 9563-9569.	13.7	116
35	Identification of the Protonated Oxygenic Ligands of Ribonucleotide Reductase Intermediate X by Q-Band1,2H CW and Pulsed ENDOR. Journal of the American Chemical Society, 1997, 119, 9816-9824.	13.7	114
36	Connecting nitrogenase intermediates with the kinetic scheme for N2 reduction by a relaxation protocol and identification of the N2 binding state. Proceedings of the National Academy of Sciences of the United States of America, 2007, 104, 1451-1455.	7.1	113

#	Article	IF	CITATIONS
37	Probing in vivo Mn <sup>2+</sup> speciation and oxidative stress resistance in yeast cells with electron-nuclear double resonance spectroscopy. Proceedings of the National Academy of Sciences of the United States of America, 2010, 107, 15335-15339.	7.1	113
38	Radical SAM catalysis via an organometallic intermediate with an Fe–[5′-C]-deoxyadenosyl bond. Science, 2016, 352, 822-825.	12.6	113
39	Spectroscopic Approaches to Elucidating Novel Ironâ^'Sulfur Chemistry in the "Radical-SAM―Protein Superfamily. Inorganic Chemistry, 2005, 44, 727-741.	4.0	108
40	Coordination and Mechanism of Reversible Cleavage of S-Adenosylmethionine by the [4Fe-4S] Center in Lysine 2,3-Aminomutase. Journal of the American Chemical Society, 2003, 125, 11788-11789.	13.7	106
41	Diazene (HNNH) Is a Substrate for Nitrogenase: Insights into the Pathway of N2Reductionâ€. Biochemistry, 2007, 46, 6784-6794.	2.5	106
42	Characterization of the nickel-iron-carbon complex formed by reaction of carbon monoxide with the carbon monoxide dehydrogenase from Clostridium thermoaceticum by Q-band ENDOR. Biochemistry, 1991, 30, 431-435.	2.5	104
43	ENDOR of the resting state of nitrogenase molybdenum-iron proteins from Azotobacter vinelandii, Klebsiella pneumoniae, and Clostridium pasteurianum. Proton, iron-57, molybdenum-95, and sulfur-33 studies. Journal of the American Chemical Society, 1986, 108, 3487-3498.	13.7	103
44	Energy Transduction in Nitrogenase. Accounts of Chemical Research, 2018, 51, 2179-2186.	15.6	101
45	Critical computational analysis illuminates the reductive-elimination mechanism that activates nitrogenase for N <sub>2</sub> reduction. Proceedings of the National Academy of Sciences of the United States of America, 2018, 115, E10521-E10530.	7.1	100
46	Identification of a Key Catalytic Intermediate Demonstrates That Nitrogenase Is Activated by the Reversible Exchange of N <sub>2</sub> for H <sub>2</sub> . Journal of the American Chemical Society, 2015, 137, 3610-3615.	13.7	99
47	Mo-, V-, and Fe-Nitrogenases Use a Universal Eight-Electron Reductive-Elimination Mechanism To Achieve N <sub>2</sub> Reduction. Biochemistry, 2019, 58, 3293-3301.	2.5	99
48	Investigation of CO bound to inhibited forms of nitrogenase MoFe protein by 13C ENDOR. Journal of the American Chemical Society, 1995, 117, 8686-8687.	13.7	98
49	Substrate Modulation of the Properties and Reactivity of the Oxy-Ferrous and Hydroperoxo-Ferric Intermediates of Cytochrome P450cam As Shown by Cryoreduction-EPR/ENDOR Spectroscopy. Journal of the American Chemical Society, 2005, 127, 1403-1413.	13.7	98
50	On reversible H <sub>2</sub> loss upon N <sub>2</sub> binding to FeMo-cofactor of nitrogenase. Proceedings of the National Academy of Sciences of the United States of America, 2013, 110, 16327-16332.	7.1	98
51	Trapping a Hydrazine Reduction Intermediate on the Nitrogenase Active Site. Biochemistry, 2005, 44, 8030-8037.	2.5	96
52	Metalloenzyme Active-Site Structure and Function through Multifrequency CW and Pulsed ENDOR. Biological Magnetic Resonance, 1993, , 151-218.	0.4	95
53	Electron transfer precedes ATP hydrolysis during nitrogenase catalysis. Proceedings of the National Academy of Sciences of the United States of America, 2013, 110, 16414-16419.	7.1	94
54	Across the tree of life, radiation resistance is governed by antioxidant Mn <sup>2+</sup> , gauged by paramagnetic resonance. Proceedings of the National Academy of Sciences of the United States of America, 2017, 114, E9253-E9260.	7.1	94

#	Article	IF	CITATIONS
55	Localization of a Substrate Binding Site on the FeMo-Cofactor in Nitrogenase:Â Trapping Propargyl Alcohol with an α-70-Substituted MoFe Proteinâ€. Biochemistry, 2003, 42, 9102-9109.	2.5	93
56	ldentification of the CO-Binding Cluster in Nitrogenase MoFe Protein by ENDOR of57Fe Isotopomers. Journal of the American Chemical Society, 1996, 118, 8707-8709.	13.7	90
57	Testing if the Interstitial Atom, <b>X</b> , of the Nitrogenase Molybdenumâ <sup>~</sup> Iron Cofactor Is N or C: ENDOR, ESEEM, and DFT Studies of the <i>S</i> = <sup>3</sup> / <sub>2</sub> Resting State in Multiple Environments. Inorganic Chemistry, 2007, 46, 11437-11449.	4.0	89
58	Evidence for Oxygen Binding at the Active Site of Particulate Methane Monooxygenase. Journal of the American Chemical Society, 2012, 134, 7640-7643.	13.7	88
59	Investigation of the Dinuclear Fe Center of Methane Monooxygenase by Advanced Paramagnetic Resonance Techniques:Â On the Geometry of DMSO Binding. Journal of the American Chemical Society, 1996, 118, 121-134.	13.7	87
60	ENDOR of Metalloenzymes. Accounts of Chemical Research, 2003, 36, 522-529.	15.6	85
61	A methyldiazene (HNNCH3)-derived species bound to the nitrogenase active-site FeMo cofactor: Implications for mechanism. Proceedings of the National Academy of Sciences of the United States of America, 2006, 103, 17113-17118.	7.1	84
62	ENDOR/HYSCORE Studies of the Common Intermediate Trapped during Nitrogenase Reduction of N <sub>2</sub> H <sub>2</sub> , CH <sub>3</sub> N <sub>2</sub> H, and N <sub>2</sub> H <sub>4</sub> Support an Alternating Reaction Pathway for N <sub>2</sub> Reduction. Journal of the American Chemical Society, 2011, 133, 11655-11664.	13.7	83
63	Rapid Freeze-Quench ENDOR Study of Chloroperoxidase Compound I:Â The Site of the Radical. Journal of the American Chemical Society, 2006, 128, 5598-5599.	13.7	82
64	Iron-57 hyperfine coupling tensors of the FeMo cluster in Azotobacter vinelandii MoFe protein: determination by polycrystalline ENDOR spectroscopy. Journal of the American Chemical Society, 1988, 110, 1935-1943.	13.7	81
65	Oxygen-17, proton, and deuterium electron nuclear double resonance characterization of solvent, substrate, and inhibitor binding to the iron-sulfur [4Fe-4S]+ cluster of aconitase. Biochemistry, 1990, 29, 10526-10532.	2.5	81
66	Mechanism of N <sub>2</sub> Reduction Catalyzed by Fe-Nitrogenase Involves Reductive Elimination of H <sub>2</sub> . Biochemistry, 2018, 57, 701-710.	2.5	80
67	Is Mo Involved in Hydride Binding by the Four-Electron Reduced (E <sub>4</sub> ) Intermediate of the Nitrogenase MoFe Protein?. Journal of the American Chemical Society, 2010, 132, 2526-2527.	13.7	79
68	Synthetic oxygen carrier. Dioxygen adduct of a manganese porphyrin. Journal of the American Chemical Society, 1975, 97, 5278-5280.	13.7	78
69	Mechanism of Radical Initiation in the Radical <i>S</i> -Adenosyl- <scp>l</scp> -methionine Superfamily. Accounts of Chemical Research, 2018, 51, 2611-2619.	15.6	78
70	Ultrafast Excited State Relaxation of a Metalloporphyrin Revealed by Femtosecond X-ray Absorption Spectroscopy. Journal of the American Chemical Society, 2016, 138, 8752-8764.	13.7	77
71	Paradigm Shift for Radical <i>S</i> -Adenosyl- <scp>l</scp> -methionine Reactions: The Organometallic Intermediate Ω Is Central to Catalysis. Journal of the American Chemical Society, 2018, 140, 8634-8638.	13.7	76
72	<sup>57</sup> Fe ENDOR Spectroscopy and â€~Electron Inventory' Analysis of the Nitrogenase E <sub>4</sub> Intermediate Suggest the Metal-Ion Core of FeMo-Cofactor Cycles Through Only One Redox Couple. Journal of the American Chemical Society, 2011, 133, 17329-17340.	13.7	75

#	Article	IF	CITATIONS
73	Generation of a Mixed-Valent Fe(III)Fe(IV) Form of Intermediate Q in the Reaction Cycle of Soluble Methane Monooxygenase, an Analog of Intermediate X in Ribonucleotide Reductase R2 Assembly. Journal of the American Chemical Society, 1998, 120, 2190-2191.	13.7	72
74	Kinetic Isotope Effects on the Rate-Limiting Step of Heme Oxygenase Catalysis Indicate Concerted Proton Transfer/Heme Hydroxylation. Journal of the American Chemical Society, 2003, 125, 16208-16209.	13.7	72
75	Chiral porphyrazine near-IR optical imaging agent exhibiting preferential tumor accumulation. Proceedings of the National Academy of Sciences of the United States of America, 2010, 107, 1284-1288.	7.1	71
76	gemini-Porphyrazines:Â The Synthesis and Characterization of Metal-Cappedcis- andtrans-Porphyrazine Tetrathiolates. Journal of the American Chemical Society, 1996, 118, 10487-10493.	13.7	70
77	Detection of two histidyl ligands to CuA of cytochrome oxidase by 35-GHz ENDOR. 14,15N and 63,65Cu ENDOR studies of the CuA site in bovine heart cytochrome aa3 and cytochromes caa3 and ba3 from Thermus thermophilus. Journal of the American Chemical Society, 1993, 115, 10888-10894.	13.7	69
78	Electron-nuclear double resonance spectroscopy (and electron spin-echo envelope modulation) Tj ETQq0 0 0 rgBT United States of America, 2003, 100, 3575-3578.	/Overlock 7.1	10 Tf 50 5 69
79	MECHANISTIC ENZYMOLOGY OF OXYGEN ACTIVATION BY THE CYTOCHROMES P450. Drug Metabolism Reviews, 2002, 34, 691-708.	3.6	68
80	The Elusive 5â€2-Deoxyadenosyl Radical: Captured and Characterized by Electron Paramagnetic Resonance and Electron Nuclear Double Resonance Spectroscopies. Journal of the American Chemical Society, 2019, 141, 12139-12146.	13.7	68
81	Trapping an Intermediate of Dinitrogen (N <sub>2</sub> ) Reduction on Nitrogenase. Biochemistry, 2009, 48, 9094-9102.	2.5	66
82	Electron Inventory, Kinetic Assignment (En), Structure, and Bonding of Nitrogenase Turnover Intermediates with C2H2and CO. Journal of the American Chemical Society, 2005, 127, 15880-15890.	13.7	65
83	Uncoupling Nitrogenase: Catalytic Reduction of Hydrazine to Ammonia by a MoFe Protein in the Absence of Fe Protein-ATP. Journal of the American Chemical Society, 2010, 132, 13197-13199.	13.7	65
84	Evidence for N coordination to Fe in the [2Fe-2S] center in yeast mitochondrial complex III Comparison with similar findings for analogous bacterial [2Fe-2S] proteins. FEBS Letters, 1987, 214, 117-121.	2.8	64
85	Responses of Mn <sup>2+</sup> speciation in <i>Deinococcus radiodurans</i> and <i>Escherichia coli</i> to γ-radiation by advanced paramagnetic resonance methods. Proceedings of the National Academy of Sciences of the United States of America, 2013, 110, 5945-5950.	7.1	63
86	Active intermediates in heme monooxygenase reactions as revealed by cryoreduction/annealing, EPR/ENDOR studies. Archives of Biochemistry and Biophysics, 2011, 507, 36-43.	3.0	62
87	Molybdenum-95 and proton ENDOR spectroscopy of the nitrogenase molybdenum-iron protein. Journal of the American Chemical Society, 1982, 104, 860-862.	13.7	61
88	An EPR Study of the Dinuclear Iron Site in the Soluble Methane Monooxygenase fromMethylococcus capsulatus(Bath) Reduced by One Electron at 77 K: The Effects of Component Interactions and the Binding of Small Molecules to the Diiron(III) Centerâ€. Biochemistry, 1999, 38, 4188-4197.	2.5	61
89	Distinct Reaction Pathways Followed upon Reduction of Oxy-Heme Oxygenase and Oxy-Myoglobin as Characterized by Mössbauer Spectroscopy. Journal of the American Chemical Society, 2007, 129, 1402-1412.	13.7	61
90	Conformational Gating of Electron Transfer from the Nitrogenase Fe Protein to MoFe Protein. Journal of the American Chemical Society, 2010, 132, 6894-6895.	13.7	61

#	Article	IF	CITATIONS
91	High-Frequency and Field EPR Investigation of (8,12-Diethyl-2,3,7,13,17,18-hexamethylcorrolato)manganese(III). Journal of the American Chemical Society, 2001, 123, 7890-7897.	13.7	60
92	Porphyrazines: Designer Macrocycles by Peripheral Substituent Change. Australian Journal of Chemistry, 2008, 61, 235.	0.9	60
93	EPR and ENDOR Characterization of the Reactive Intermediates in the Generation of NO by Cryoreduced Oxy-Nitric Oxide Synthase from <i>Geobacillus stearothermophilus</i> . Journal of the American Chemical Society, 2009, 131, 14493-14507.	13.7	60
94	Reversible Photoinduced Reductive Elimination of H <sub>2</sub> from the Nitrogenase Dihydride State, the E <sub>4</sub> (4H) Janus Intermediate. Journal of the American Chemical Society, 2016, 138, 1320-1327.	13.7	60
95	Triplet Exciton EPR and Crystal Structure of [TMPD+]2[Ni(mnt)2]â^'2. Journal of Chemical Physics, 1972, 56, 3490-3502.	3.0	59
96	Substrate Binding to NOâ^'Ferroâ^'Naphthalene 1,2-Dioxygenase Studied by High-Resolution Q-Band Pulsed2H-ENDOR Spectroscopy. Journal of the American Chemical Society, 2003, 125, 7056-7066.	13.7	59
97	Unification of reaction pathway and kinetic scheme for N <sub>2</sub> reduction catalyzed by nitrogenase. Proceedings of the National Academy of Sciences of the United States of America, 2012, 109, 5583-5587.	7.1	59
98	Why Nature Uses Radical SAM Enzymes so Widely: Electron Nuclear Double Resonance Studies of Lysine 2,3-Aminomutase Show the 5′-dAdo• "Free Radical―Is Never Free. Journal of the American Chemical Society, 2015, 137, 7111-7121.	13.7	59
99	High-Resolution ENDOR Spectroscopy Combined with Quantum Chemical Calculations Reveals the Structure of Nitrogenase Janus Intermediate E <sub>4</sub> (4H). Journal of the American Chemical Society, 2019, 141, 11984-11996.	13.7	58
100	A Superoxo-Ferrous State in a Reduced Oxy-Ferrous Hemoprotein and Model Compounds. Journal of the American Chemical Society, 2003, 125, 16340-16346.	13.7	57
101	EPR and ENDOR Studies of Cryoreduced Compounds II of Peroxidases and Myoglobin. Proton-Coupled Electron Transfer and Protonation Status of Ferryl Hemes. Biochemistry, 2008, 47, 5147-5155.	2.5	57
102	Structure of the Nucleotide Radical Formed during Reaction of CDP/TTP with the E441Q-α2β2 of <i>E. coli</i> Ribonucleotide Reductase. Journal of the American Chemical Society, 2009, 131, 200-211.	13.7	55
103	Experimental and Theoretical EPR Study of Jahnâ^'Teller-Active [HIPTN <sub>3</sub> N]MoL Complexes (L) Tj ETC	2q110.78 13.7	4314 rgBT
104	The dioxygen adducts of several manganese(II) porphyrins. Electron paramagnetic resonance studies. Journal of the American Chemical Society, 1978, 100, 7253-7259.	13.7	54
105	Making hyperfine selection in Mims ENDOR independent of deadtime. Chemical Physics Letters, 1997, 269, 208-214.	2.6	53
106	Manganese co-localizes with calcium and phosphorus in Chlamydomonas acidocalcisomes and is mobilized in manganese-deficient conditions. Journal of Biological Chemistry, 2019, 294, 17626-17641.	3.4	53
107	Cytochrome c Peroxidaseâ^'Cytochrome c Complex:  Locating the Second Binding Domain on Cytochrome c Peroxidase with Site-Directed Mutagenesis. Biochemistry, 2000, 39, 10132-10139.	2.5	52
108	Functional solitare- and trans-hybrids, the synthesis, characterization, electrochemistry and reactivity of porphyrazine/phthalocyanine hybrids bearing nitro and amino functionality. Journal of Porphyrins and Phthalocyanines, 2003, 07, 700-712.	0.8	52

#	Article	IF	CITATIONS
109	EPR, ENDOR, and Electronic Structure Studies of the Jahn–Teller Distortion in an FeVNitride. Journal of the American Chemical Society, 2014, 136, 12323-12336.	13.7	52
110	Studies on seco-porphyrazines: a case study on serendipity. Dalton Transactions, 2003, , 2093.	3.3	51
111	Differential influence of dynamic processes on forward and reverse electron transfer across a protein-protein interface. Proceedings of the National Academy of Sciences of the United States of America, 2005, 102, 3564-3569.	7.1	51
112	Synthesis and Characterization of New Porphyrazine-Gd(III) Conjugates as Multimodal MR Contrast Agents. Bioconjugate Chemistry, 2010, 21, 2267-2275.	3.6	51
113	Mechanism of Nitrogenase H <sub>2</sub> Formation by Metal-Hydride Protonation Probed by Mediated Electrocatalysis and H/D Isotope Effects. Journal of the American Chemical Society, 2017, 139, 13518-13524.	13.7	51
114	Characterization of an Intermediate in the Reduction of Acetylene by the Nitrogenase α-Gln195MoFe Protein by Q-band EPR and13C,1H ENDOR. Journal of the American Chemical Society, 2000, 122, 5582-5587.	13.7	50
115	Identification of the Valence and Coordination Environment of the Particulate Methane Monooxygenase Copper Centers by Advanced EPR Characterization. Journal of the American Chemical Society, 2014, 136, 11767-11775.	13.7	49
116	From micelles to bicelles: Effect of the membrane on particulate methane monooxygenase activity. Journal of Biological Chemistry, 2018, 293, 10457-10465.	3.4	49
117	Calculation of z-Coordinates and Orientational Restraints Using a Metal Binding Tag. Biochemistry, 2000, 39, 15217-15224.	2.5	48
118	Organometallic and radical intermediates reveal mechanism of diphthamide biosynthesis. Science, 2018, 359, 1247-1250.	12.6	48
119	Characterization of the Microsomal Cytochrome P450 2B4 O2 Activation Intermediates by Cryoreduction and Electron Paramagnetic Resonance. Biochemistry, 2008, 47, 9661-9666.	2.5	47
120	CO <sub>2</sub> Reduction Catalyzed by Nitrogenase: Pathways to Formate, Carbon Monoxide, and Methane. Inorganic Chemistry, 2016, 55, 8321-8330.	4.0	47
121	<sup>13</sup> C ENDOR Spectroscopy of Lipoxygenase–Substrate Complexes Reveals the Structural Basis for C–H Activation by Tunneling. Journal of the American Chemical Society, 2017, 139, 1984-1997.	13.7	47
122	Probing the Ternary Complexes of Indoleamine and Tryptophan 2,3-Dioxygenases by Cryoreduction EPR and ENDOR Spectroscopy. Journal of the American Chemical Society, 2010, 132, 5494-5500.	13.7	46
123	Characterization of a long overlooked copper protein from methane- and ammonia-oxidizing bacteria. Nature Communications, 2018, 9, 4276.	12.8	46
124	Interaction of Acetylene and Cyanide with the Resting State of Nitrogenase α-96-Substituted MoFe Proteins. Biochemistry, 2001, 40, 13816-13825.	2.5	45
125	Detection of a new signal in the ESR spectrum of vanadium nitrogenase from Azotobacter vinelandii. Journal of the American Chemical Society, 1989, 111, 8519-8520.	13.7	44
126	Kinetic Understanding of N <sub>2</sub> Reduction versus H <sub>2</sub> Evolution at the E <sub>4</sub> (4H) Janus State in the Three Nitrogenases. Biochemistry, 2018, 57, 5706-5714.	2.5	44

#	Article	IF	CITATIONS
127	General theory of polycrystalline ENDOR patterns. g and hyperfine tensors of arbitrary symmetry and relative orientation. Journal of Magnetic Resonance, 1984, 59, 110-123.	0.5	43
128	Compound I Is the Reactive Intermediate in the First Monooxygenation Step during Conversion of Cholesterol to Pregnenolone by Cytochrome P450scc: EPR/ENDOR/Cryoreduction/Annealing Studies. Journal of the American Chemical Society, 2012, 134, 17149-17156.	13.7	43
129	Control of electron transfer in nitrogenase. Current Opinion in Chemical Biology, 2018, 47, 54-59.	6.1	43
130	Negative cooperativity in the nitrogenase Fe protein electron delivery cycle. Proceedings of the National Academy of Sciences of the United States of America, 2016, 113, E5783-E5791.	7.1	42
131	Photoinduced Reductive Elimination of H <sub>2</sub> from the Nitrogenase Dihydride (Janus) State Involves a FeMo-cofactor-H <sub>2</sub> Intermediate. Inorganic Chemistry, 2017, 56, 2233-2240.	4.0	42
132	[23] Protein structure and mechanism studied by electron nuclear double resonance spectroscopy. Methods in Enzymology, 1995, 246, 554-589.	1.0	41
133	Enantiomerically Pure"Winged―Spirane Porphyrazinoctaols. Angewandte Chemie International Edition in English, 1997, 36, 760-761.	4.4	40
134	Nitrogenase Reduction of Carbon Disulfide:Â Freeze-Quench EPR and ENDOR Evidence for Three Sequential Intermediates with Cluster-Bound Carbon Moietiesâ€. Biochemistry, 2000, 39, 1114-1119.	2.5	40
135	Peripherally Functionalized Porphyrazines: Novel Metallomacrocycles with Broad, Untapped Potential. Progress in Inorganic Chemistry, 2002, , 473-590.	3.0	40
136	A Confirmation of the Quench-Cryoannealing Relaxation Protocol for Identifying Reduction States of Freeze-Trapped Nitrogenase Intermediates. Inorganic Chemistry, 2014, 53, 3688-3693.	4.0	40
137	Structural and spectroscopic characterization of an Fe(VI) bis(imido) complex. Science, 2020, 370, 356-359.	12.6	40
138	Jahn-Teller effects in metalloporphyrins and other four-fold symmetric systems. Molecular Physics, 1978, 35, 901-925.	1.7	39
139	Porphyrazinediols:  Synthesis, Characterization, and Complexation to Group IVB Metallocenes. Journal of Organic Chemistry, 2000, 65, 1774-1779.	3.2	38
140	Modeling the Signatures of Hydrides in Metalloenzymes: ENDOR Analysis of a Di-iron Fe(μ-NH)(μ-H)Fe Core. Journal of the American Chemical Society, 2012, 134, 12637-12647.	13.7	38
141	Spectroscopic Description of the E <sub>1</sub> State of Mo Nitrogenase Based on Mo and Fe X-ray Absorption and Mössbauer Studies. Inorganic Chemistry, 2019, 58, 12365-12376.	4.0	38
142	Comparison of wild-type and nifV mutant molybdenum-iron proteins of nitrogenase from Klebsiella pneumoniae by ENDOR spectroscopy. Journal of the American Chemical Society, 1990, 112, 651-657.	13.7	37
143	Photoinduced Electron Transfer between CytochromecPeroxidase (D37K) and Zn-Substituted Cytochromec:Â Probing the Two-Domain Binding and Reactivity of the Peroxidase. Journal of the American Chemical Society, 1997, 119, 269-277.	13.7	37
144	Structure of the Modified Heme in Allylbenzene-Inactivated Chloroperoxidase Determined by Q-Band CW and Pulsed ENDOR. Journal of the American Chemical Society, 1997, 119, 4059-4069.	13.7	37

#	Article	IF	CITATIONS
145	Paramagnetic Intermediates of ( <i>E</i> )-4-Hydroxy-3-methylbut-2-enyl Diphosphate Synthase (GcpE/IspG) under Steady-State and Pre-Steady-State Conditions. Journal of the American Chemical Society, 2010, 132, 14509-14520.	13.7	37
146	Cryogenic Electron Tunneling within Mixed-Metal Hemoglobin Hybrids:Â Protein Glassing and Electron-Transfer Energetics. Journal of the American Chemical Society, 1998, 120, 11401-11407.	13.7	36
147	Nitrogen-14 and oxygen-17 hyperfine interactions in perturbed nitroxides. The Journal of Physical Chemistry, 1974, 78, 1313-1321.	2.9	34
148	Advanced paramagnetic resonance spectroscopies of iron–sulfur proteins: Electron nuclear double resonance (ENDOR) and electron spin echo envelope modulation (ESEEM). Biochimica Et Biophysica Acta - Molecular Cell Research, 2015, 1853, 1370-1394.	4.1	34
149	Characterization of Methanobactin from <i>Methylosinus</i> sp. LW4. Journal of the American Chemical Society, 2016, 138, 11124-11127.	13.7	34
150	Nitrite and Hydroxylamine as Nitrogenase Substrates: Mechanistic Implications for the Pathway of N2 Reduction. Journal of the American Chemical Society, 2014, 136, 12776-12783.	13.7	33
151	Free H <sub>2</sub> Rotation vs Jahn–Teller Constraints in the Nonclassical Trigonal (TPB)Co–H <sub>2</sub> Complex. Journal of the American Chemical Society, 2014, 136, 14998-15009.	13.7	33
152	Evidence That Compound I Is the Active Species in Both the Hydroxylase and Lyase Steps by Which P450scc Converts Cholesterol to Pregnenolone: EPR/ENDOR/Cryoreduction/Annealing Studies. Biochemistry, 2015, 54, 7089-7097.	2.5	33
153	Conformational Substates of the Oxyheme Centers in α and β Subunits of Hemoglobin As Disclosed by EPR and ENDOR Studies of Cryoreduced Proteinâ€. Biochemistry, 2004, 43, 6330-6338.	2.5	32
154	A structurally-characterized peroxomanganese( <scp>iv</scp> ) porphyrin from reversible O <sub>2</sub> binding within a metal–organic framework. Chemical Science, 2018, 9, 1596-1603.	7.4	32
155	Electron Redistribution within the Nitrogenase Active Site FeMo-Cofactor During Reductive Elimination of H <sub>2</sub> to Achieve N≡N Triple-Bond Activation. Journal of the American Chemical Society, 2020, 142, 21679-21690.	13.7	32
156	Structure of Nitric Oxide Adsorbed on 4A Molecular Sieve. Journal of Chemical Physics, 1969, 50, 2598-2603.	3.0	31
157	Tumbling of an adsorbed nitroxide using rapid adiabatic passage. The Journal of Physical Chemistry, 1976, 80, 842-846.	2.9	31
158	Formation of {[HIPTN <sub>3</sub> N]Mo(III)H} <sup>â^'</sup> by Heterolytic Cleavage of H <sub>2</sub> as Established by EPR and ENDOR Spectroscopy. Inorganic Chemistry, 2010, 49, 704-713.	4.0	31
159	Cu <sup>+</sup> -specific CopB transporter: Revising P <sub>1B</sub> -type ATPase classification. Proceedings of the National Academy of Sciences of the United States of America, 2018, 115, 2108-2113.	7.1	31
160	Photoinduced Electron Transfer in a Radical SAM Enzyme Generates an <i>S</i> -Adenosylmethionine Derived Methyl Radical. Journal of the American Chemical Society, 2019, 141, 16117-16124.	13.7	31
161	Spectroscopic and Crystallographic Evidence for the Role of a Water-Containing H-Bond Network in Oxidase Activity of an Engineered Myoglobin. Journal of the American Chemical Society, 2016, 138, 1134-1137.	13.7	30
162	Photocurrent from photocorrosion of aluminum electrode in porphyrin/Al Schottky-barrier cells. Applied Physics Letters, 1997, 71, 674-676.	3.3	29

#	Article	IF	CITATIONS
163	Simulating Suppression Effects in Pulsed ENDOR, and the â€~Hole in the Middle' of Mims and Davies ENDOR Spectra. Applied Magnetic Resonance, 2010, 37, 763-779.	1.2	29
164	Hydride Conformers of the Nitrogenase FeMo-cofactor Two-Electron Reduced State E <sub>2</sub> (2H), Assigned Using Cryogenic Intra Electron Paramagnetic Resonance Cavity Photolysis. Inorganic Chemistry, 2018, 57, 6847-6852.	4.0	29
165	Comment on "Structural evidence for a dynamic metallocofactor during N <sub>2</sub> reduction by Mo-nitrogenase― Science, 2021, 371, .	12.6	29
166	ELECTRON NUCLEAR DOUBLE RESONANCE (ENDOR) OF METALLOENZYMES. , 1989, , 541-591.		29
167	Porphyrinic Molecular Metals. Molecular Crystals and Liquid Crystals, 1985, 125, 1-11.	0.8	28
168	Monovalent Cation Activation of the Radical SAM Enzyme Pyruvate Formate-Lyase Activating Enzyme. Journal of the American Chemical Society, 2017, 139, 11803-11813.	13.7	28
169	EPR Study of the Low-Spin [d3; S =1/2], Jahnâ^'Teller-Active, Dinitrogen Complex of a Molybdenum Trisamidoamine. Journal of the American Chemical Society, 2007, 129, 3480-3481.	13.7	27
170	Characterization of a Cobalt-Specific P <sub>1B</sub> -ATPase. Biochemistry, 2012, 51, 7891-7900.	2.5	27
171	Interaction of Tl+ and Cs+ with the [Fe3S4] Cluster of Pyrococcus furiosus Ferredoxin: Investigation by Resonance Raman, MCD, EPR, and ENDOR Spectroscopy. Journal of the American Chemical Society, 1994, 116, 5722-5729.	13.7	26
172	The Use of Deuterated Camphor as a Substrate in <sup>1</sup> H ENDOR Studies of Hydroxylation by Cryoreduced Oxy P450cam Provides New Evidence of the Involvement of Compound I. Biochemistry, 2013, 52, 667-671.	2.5	26
173	The C-Terminal Heme Regulatory Motifs of Heme Oxygenase-2 Are Redox-Regulated Heme Binding Sites. Biochemistry, 2015, 54, 2709-2718.	2.5	26
174	Role of the Proximal Cysteine Hydrogen Bonding Interaction in Cytochrome P450 2B4 Studied by Cryoreduction, Electron Paramagnetic Resonance, and Electron–Nuclear Double Resonance Spectroscopy. Biochemistry, 2016, 55, 869-883.	2.5	26
175	Binding and Electron Transfer between Cytochromeb5and the Hemoglobin α- and β-Subunits through the Use of [Zn, Fe] Hybrids. Journal of the American Chemical Society, 1998, 120, 11256-11262.	13.7	25
176	Griffith model bonding in dioxygen complexes of manganese porphyrins. Journal of the American Chemical Society, 1980, 102, 4602-4609.	13.7	24
177	Tuning the Singlet Oxygen Quantum Yield of Near-IR–absorbing Porphyrazines¶. Photochemistry and Photobiology, 2003, 77, 18.	2.5	24
178	Identification of a Hemerythrin-like Domain in a P <sub>1B</sub> -Type Transport ATPase. Biochemistry, 2010, 49, 7060-7068.	2.5	24
179	Coordination of the Copper Centers in Particulate Methane Monooxygenase: Comparison between Methanotrophs and Characterization of the Cu <sub>C</sub> Site by EPR and ENDOR Spectroscopies. Journal of the American Chemical Society, 2021, 143, 15358-15368.	13.7	24
180	Investigation of exchange couplings in [Fe3S4]+ clusters by electron spin-lattice relaxation. Journal of Biological Inorganic Chemistry, 2000, 5, 369-380.	2.6	22

#	Article	IF	CITATIONS
181	Chiral <i>bis</i> â€Acetal Porphyrazines as Nearâ€infrared Optical Agents for Detection and Treatment of Cancer. Photochemistry and Photobiology, 2010, 86, 410-417.	2.5	22
182	Organometallic Complex Formed by an Unconventional Radical <i>S</i> -Adenosylmethionine Enzyme. Journal of the American Chemical Society, 2016, 138, 9755-9758.	13.7	21
183	Composition and Structure of the Inorganic Core of Relaxed Intermediate <b>X</b> (Y122F) of <i>Escherichia coli</i> Ribonucleotide Reductase. Journal of the American Chemical Society, 2015, 137, 15558-15566.	13.7	20
184	Metal Selectivity of a Cd-, Co-, and Zn-Transporting P <sub>1B</sub> -type ATPase. Biochemistry, 2017, 56, 85-95.	2.5	20
185	Versatile fourâ€probe ac conductivity measurement system. Review of Scientific Instruments, 1979, 50, 263-265.	1.3	19
186	Lanthanide porphyrazine sandwich complexes: synthetic, structural and spectroscopic investigations. Dalton Transactions RSC, 2001, , 3269-3273.	2.3	19
187	Substrate-Dependent Cleavage Site Selection by Unconventional Radical <i>S</i> -Adenosylmethionine Enzymes in Diphthamide Biosynthesis. Journal of the American Chemical Society, 2017, 139, 5680-5683.	13.7	19
188	<i>S</i> â€Adenosylâ€ <scp>l</scp> â€ethionine is a Catalytically Competent Analog of <i>S</i> â€Adenosylâ€ <scp>l</scp> â€methionine (SAM) in the Radical SAM Enzyme HydG. Angewandte Chemie - International Edition, 2021, 60, 4666-4672.	13.8	19
189	An ecophysiological explanation for manganese enrichment in rock varnish. Proceedings of the National Academy of Sciences of the United States of America, 2021, 118, .	7.1	19
190	Formation and Electronic Structure of an Atypical Cu <sub>A</sub> Site. Journal of the American Chemical Society, 2019, 141, 4678-4686.	13.7	18
191	CO as a substrate and inhibitor of H+ reduction for the Mo-, V-, and Fe-nitrogenase isozymes. Journal of Inorganic Biochemistry, 2020, 213, 111278.	3.5	18
192	Metal ion fluxes controlling amphibian fertilization. Nature Chemistry, 2021, 13, 683-691.	13.6	18
193	<b>Mechanism of Radical <i>S</i>-Adenosyl-</b> <scp> </scp> -methionine Adenosylation: Radical Intermediates and the Catalytic Competence of the 5′-Deoxyadenosyl Radical. Journal of the American Chemical Society, 2022, 144, 5087-5098.	13.7	18
194	Cobalt–Carbon Bonding in a Salen-Supported Cobalt(IV) Alkyl Complex Postulated in Oxidative MHAT Catalysis. Journal of the American Chemical Society, 2022, 144, 10361-10367.	13.7	18
195	Multi-gram synthesis of a porphyrazine platform for cellular translocation, conjugation to Doxorubicin, and cellular uptake. Tetrahedron Letters, 2012, 53, 5475-5478.	1.4	17
196	The Soybean Lipoxygenase–Substrate Complex: Correlation between the Properties of Tunneling-Ready States and ENDOR-Detected Structures of Ground States. Biochemistry, 2020, 59, 901-910.	2.5	17
197	The electronic structure of FeV-cofactor in vanadium-dependent nitrogenase. Chemical Science, 2021, 12, 6913-6922.	7.4	17
198	End-On Copper(I) Superoxo and Cu(II) Peroxo and Hydroperoxo Complexes Generated by Cryoreduction/Annealing and Characterized by EPR/ENDOR Spectroscopy. Journal of the American Chemical Society, 2022, 144, 377-389.	13.7	17

#	Article	IF	CITATIONS
199	Synthesis and characterization of a porphyrazine–Gd(III) MRI contrast agent and <i>in vivo</i> imaging of a breast cancer xenograft model. Contrast Media and Molecular Imaging, 2014, 9, 313-322.	0.8	16
200	Carrier Properties of Porphyrinic Molecular Metals. Molecular Crystals and Liquid Crystals, 1982, 81, 231-242.	0.8	15
201	Synthesis, Characterization and Reactions of Enantiomerically Pure †Winged' Spirane Porphyrazines. Tetrahedron, 2000, 56, 6565-6569.	1.9	15
202	Spectroscopic Studies Reveal That the Heme Regulatory Motifs of Heme Oxygenase-2 Are Dynamically Disordered and Exhibit Redox-Dependent Interaction with Heme. Biochemistry, 2015, 54, 2693-2708.	2.5	15
203	Isolation and characterization of a high-spin mixed-valent iron dinitrogen complex. Chemical Communications, 2018, 54, 13339-13342.	4.1	15
204	Active-Site Controlled, Jahn–Teller Enabled Regioselectivity in Reductive S–C Bond Cleavage of <i>S</i> -Adenosylmethionine in Radical SAM Enzymes. Journal of the American Chemical Society, 2021, 143, 335-348.	13.7	15
205	ENDOR Spectroscopic Evidence for the Geometry of Binding ofretro-inverso-NI‰-Nitroarginine-Containing Dipeptide Amides to Neuronal Nitric Oxide Synthase. Journal of the American Chemical Society, 2000, 122, 7869-7875.	13.7	14
206	Electron Paramagnetic Resonance and Electron-Nuclear Double Resonance Studies of the Reactions of Cryogenerated Hydroperoxoferric–Hemoprotein Intermediates. Biochemistry, 2014, 53, 4894-4903.	2.5	14
207	EPR/ENDOR and Theoretical Study of the Jahn–Teller-Active [HIPTN <sub>3</sub> N]Mo <sup>V</sup> L Complexes (L = N <sup>–</sup> , NH). Inorganic Chemistry, 2017, 56, 6906-6919.	4.0	14
208	Hydrocarbon Oxidation by an Exposed, Multiply Bonded Iron(III) Oxo Complex. ACS Central Science, 2021, 7, 1751-1755.	11.3	14
209	A mixed-valent Fe(II)Fe(III) species converts cysteine to an oxazolone/thioamide pair in methanobactin biosynthesis. Proceedings of the National Academy of Sciences of the United States of America, 2022, 119, e2123566119.	7.1	14
210	Synthesis and characterization of periphery-functionalized porphyrazines containing mixed pyrrolyl and pyridylmethylamino groups. Journal of Porphyrins and Phthalocyanines, 2009, 13, 223-234.	0.8	13
211	Exploring Electron/Proton Transfer and Conformational Changes in the Nitrogenase MoFe Protein and FeMoâ€cofactor Through Cryoreduction/EPR Measurements. Israel Journal of Chemistry, 2016, 56, 841-851.	2.3	13
212	Exploring the Role of the Central Carbide of the Nitrogenase Active-Site FeMo-cofactor through Targeted <sup>13</sup> C Labeling and ENDOR Spectroscopy. Journal of the American Chemical Society, 2021, 143, 9183-9190.	13.7	13
213	[FeFe]â€Hydrogenase: Defined Lysateâ€Free Maturation Reveals a Key Role for Lipoylâ€Hâ€Protein in DTMA Ligand Biosynthesis. Angewandte Chemie - International Edition, 2022, 61, .	13.8	13
214	Temperature Invariance of the Nitrogenase Electron Transfer Mechanism. Biochemistry, 2012, 51, 8391-8398.	2.5	12
215	ENDOR Characterization of (N <sub>2</sub> )Fe <sup>II</sup> (μ-H) <sub>2</sub> Fe <sup>I</sup> (N <sub>2</sub> ) <sup>â^`</sup> : A Spectroscopic Model for N <sub>2</sub> Binding by the Di-μ-hydrido Nitrogenase Janus Intermediate. Inorganic Chemistry, 2018, 57, 12323-12330.	4.0	12
216	Time-Resolved EPR Study of H <sub>2</sub> Reductive Elimination from the Photoexcited Nitrogenase	2.6	12

#	Article	IF	CITATIONS
217	Small-Molecule Mn Antioxidants in Caenorhabditis elegans and Deinococcus radiodurans Supplant MnSOD Enzymes during Aging and Irradiation. MBio, 2022, 13, e0339421.	4.1	12
218	The One-Electron Reduced Active-Site FeFe-Cofactor of Fe-Nitrogenase Contains a Hydride Bound to a Formally Oxidized Metal-Ion Core. Inorganic Chemistry, 2022, 61, 5459-5464.	4.0	12
219	PCuAC domains from methane-oxidizing bacteria use a histidine brace to bind copper. Journal of Biological Chemistry, 2019, 294, 16351-16363.	3.4	11
220	Energetics and Dynamics of Gated Reactions. Advances in Chemistry Series, 1989, , 125-146.	0.6	10
221	Multi-domain binding of cytochromecperoxidase by cytochromec: Thermodynamic vs. microscopic binding constants. Israel Journal of Chemistry, 2000, 40, 35-46.	2.3	10
222	Effects of substrates (methyl isocyanide, C2H2) and inhibitor (CO) on resting-state wild-type and NifVâ^'Klebsiella pneumoniae MoFe proteins. Journal of Inorganic Biochemistry, 2003, 93, 18-32.	3.5	10
223	Design, Implementation, Simulation, and Visualization of a Highly Efficient RIM Microfluidic Mixer for Rapid Freeze-Quench of Biological Samples. Applied Magnetic Resonance, 2011, 40, 415-425.	1.2	10
224	Imaging ultrafast excited state pathways in transition metal complexes by X-ray transient absorption and scattering using X-ray free electron laser source. Faraday Discussions, 2016, 194, 639-658.	3.2	10
225	Radical SAM Enzyme Spore Photoproduct Lyase: Properties of the Ω Organometallic Intermediate and Identification of Stable Protein Radicals Formed during Substrate-Free Turnover. Journal of the American Chemical Society, 2020, 142, 18652-18660.	13.7	10
226	Interplays of electron and nuclear motions along CO dissociation trajectory in myoglobin revealed by ultrafast X-rays and quantum dynamics calculations. Proceedings of the National Academy of Sciences of the United States of America, 2021, 118, .	7.1	10
227	Long-Range Electron Transfer Within Mixed-Metal Hemoglobin Hybrids. Advances in Chemistry Series, 1991, , 201-213.	0.6	9
228	Comparison of the Mechanisms of Heme Hydroxylation by Heme Oxygenases-1 and -2: Kinetic and Cryoreduction Studies. Biochemistry, 2016, 55, 62-68.	2.5	9
229	<sup>13</sup> C Electron Nuclear Double Resonance Spectroscopy Shows Acetyl-CoA Synthase Binds Two Substrate CO in Multiple Binding Modes and Reveals the Importance of a CO-Binding "Alcoveâ€ Journal of the American Chemical Society, 2020, 142, 15362-15370.	13.7	9
230	ENDOR characterization of an iron–alkene complex provides insight into a corresponding organometallic intermediate of nitrogenase. Chemical Science, 2017, 8, 5941-5948.	7.4	8
231	Copper binding by a unique family of metalloproteins is dependent on kynurenine formation. Proceedings of the National Academy of Sciences of the United States of America, 2021, 118, .	7.1	8
232	Insights into the Role of Nickel in Hydrogenase. Advances in Chemistry Series, 1996, , 21-60.	0.6	7
233	Q-Band ENDOR Studies of the Nitrogenase MoFe Protein under Turnover Conditions. ACS Symposium Series, 2003, , 150-178.	0.5	7
234	The Role of Co-ZSM-5 Catalysts in Aerobic Oxidation of Ethylbenzene. Topics in Catalysis, 2020, 63, 1708-1716.	2.8	7

#	Article	IF	CITATIONS
235	Ferromagnetism in a New Structural, Phase of [Fe(C5Me5)2] [TCNQ]. Molecular Crystals and Liquid Crystals, 1995, 273, 17-20.	0.3	6
236	MbnH is a diheme MauG-like protein associated with microbial copper homeostasis. Journal of Biological Chemistry, 2019, 294, 16141-16151.	3.4	6
237	An Engineered Glutamate in Biosynthetic Models of Heme-Copper Oxidases Drives Complete Product Selectivity by Tuning the Hydrogen-Bonding Network. Biochemistry, 2021, 60, 346-355.	2.5	6
238	Tuning the Singlet Oxygen Quantum Yield of Near-IR-absorbing Porphyrazines¶. Photochemistry and Photobiology, 2003, 77, 18-21.	2.5	5
239	Charge-Disproportionation Symmetry Breaking Creates a Heterodimeric Myoglobin Complex with Enhanced Affinity and Rapid Intracomplex Electron Transfer. Journal of the American Chemical Society, 2016, 138, 12615-12628.	13.7	5
240	[FeFe]â€Hydrogenase: Defined Lysateâ€Free Maturation Reveals a Key Role for Lipoylâ€Hâ€Protein in DTMA Ligand Biosynthesis. Angewandte Chemie, 2022, 134, .	2.0	5
241	Allosteric Control of O2 Reactivity in Rieske Oxygenases. Structure, 2005, 13, 684-685.	3.3	3
242	<i>S</i> â€Adenosylâ€ <scp>l</scp> â€ethionine is a Catalytically Competent Analog of <i>S</i> â€Adenosylâ€ <scp>l</scp> â€methionine (SAM) in the Radical SAM Enzyme HydG. Angewandte Chemie, 2021, 133, 4716-4722.	2.0	3
243	Single-crystal EPR and ENDOR study of nitrogenase from clostridium pasteurianum. Journal of Magnetic Resonance, 1991, 91, 227-240.	0.5	2
244	Structure Determination by Combination of CW and Pulsed '2-D' Orientation-Selective 1,2H Q-Band Electron-Nuclear Double Resonance. ACS Symposium Series, 1998, , 2-15.	0.5	1
245	Discovery of the Antitumor Effects of a Porphyrazine Diol (Pz 285) in MDA-MB-231 Breast Tumor Xenograft Models in Mice. ACS Medicinal Chemistry Letters, 2017, 8, 705-709.	2.8	1
246	Evidence Regarding Mechanisms for Protein Control of Heme Reactivity. Advances in Chemistry Series, 1980, , 235-252.	0.6	0
247	Enantiomerenreine schaufelradartige Spiroâ€Porphyrazinoctaolderivate. Angewandte Chemie, 1997, 109, 806-807.	2.0	0
248	Paramagnetic Resonance in Mechanistic Studies of Fe-S/Radical Enzymes. ACS Symposium Series, 2003, , 113-127.	0.5	0
249	Tuning the Singlet Oxygen Quantum Yield of Near-IR-absorbing Porphyrazines. Photochemistry and Photobiology, 2007, 78, 645-645.	2.5	0
250	Short-lived neutral FMN and FAD semiquinones are transient intermediates in cryo-reduced yeast NADPH-cytochrome P450 reductase. Archives of Biochemistry and Biophysics, 2019, 673, 108080.	3.0	0
251	Structure, reactivity and function of bacterial nitric oxide synthases. FASEB Journal, 2009, 23, .	0.5	0
252	A New Reaction for Improved Calibration of EPR Rapid-Freeze Quench Times: Kinetics of Ethylene Diamine Tetraacetate (EDTA) Transfer from Calcium(II) to Copper(II). Applied Magnetic Resonance, 0, , 1.	1.2	0

#	Article	IF	CITATIONS
253	Titelbild: [FeFe]â€Hydrogenase: Defined Lysateâ€Free Maturation Reveals a Key Role for Lipoylâ€Hâ€Protein in DTMA Ligand Biosynthesis (Angew. Chem. 22/2022). Angewandte Chemie, 2022, 134, .	2.0	0